Instrumentation for the non-destructive optical measurement of trapped electrons in feldspar

Kook, M.; Kumar, R.; Murray, A.S.; Thomsen, K.J.; Jain, M.

Published in:
Radiation Measurements

Link to article, DOI:
10.1016/j.radmeas.2018.06.001

Publication date:
2018

Document Version
Peer reviewed version

Accepted Manuscript

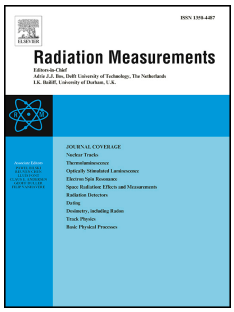

Instrumentation for the non-destructive optical measurement of trapped electrons in feldspar

M. Kook, R. Kumar, A.S. Murray, K.J. Thomsen, M. Jain

PII: S1350-4487(17)30859-4

DOI: 10.1016/j.radmeas.2018.06.001

Reference: RM 5923

To appear in: *Radiation Measurements*

Received Date: 13 December 2017

Revised Date: 19 March 2018

Accepted Date: 2 June 2018

Please cite this article as: Kook, M., Kumar, R., Murray, A.S., Thomsen, K.J., Jain, M., Instrumentation for the non-destructive optical measurement of trapped electrons in feldspar, *Radiation Measurements* (2018), doi: 10.1016/j.radmeas.2018.06.001.

Instrumentation for the non-destructive optical measurement of trapped electrons in feldspar

M. Kook[1]*, R. Kumar[1], A.S. Murray[2], K.J. Thomsen[1], M. Jain[1]

*Corresponding author: myko@dtu.dk

[1]Center for Nuclear Technologies, Technical University of Denmark, DTU Risø Campus, DK-4000 Roskilde, Denmark

[2]Nordic Laboratory for Luminescence Dating, Department of Geoscience, Aarhus University, Risø Campus, DK-4000 Roskilde, Denmark

Abstract

A facility for the measurement of infrared photoluminescence (IRPL) has been developed for the Risø TL/OSL reader. The new IRPL measurement system uses an external laser light source at 1.49 eV (830 nm) and two photomultiplier tubes (PMT) for detecting emissions at ~1.41 eV (880 nm) and ~1.3 eV (955 nm) and an EMCCD. Pulsed IRPL measurement ensures a low background count rate by allowing the rejection of breakthrough from excitation light. We present the results of integrated IRPL measurements on both multiple- and single-grain aliquots, and finally demonstrate the potential of imaging natural K-feldspar samples and a granite rock slice.

Keywords: Infrared photoluminescence (IRPL), Feldspar, Single grain, Imaging, Optical dating

1. Introduction

Optically stimulated luminescence (OSL) emission arises from recombination of trapped electrons and holes in a crystal due to stimulation by light of appropriate energy; this signal is dose dependent and always measured in the anti-Stokes mode to avoid contamination from prompt fluorescence and phosphorescence emissions (Bøtter-Jensen et al., 2003). OSL decays during stimulation because luminescence emission is the result of progressive release of charge from traps followed by electron-hole recombination. In contrast, infrared photoluminescence (IRPL), detected for the first time in feldspar at ~955 nm during IR excitation at (885 nm) by Prasad et al. (2017), is a Stokes shifted emission resulting from internal excitation-relaxation within the dosimetric trap (henceforth principal trap). Kumar et al. (these proceedings) have discovered a second IRPL emission at ~880 nm using a shorter wavelength excitation at 830 nm in a potassium rich feldspar. IRPL does not involve release of charge from traps, nor does it require hole-centres to produce luminescence; the signal can thus be accumulated over long periods by repeated excitation of the same trapped electron, without significant signal loss. This is especially true for electron traps with a large distance to the nearest recombination site (i.e. non-fading traps) or measurements done at cryogenic temperatures (Prasad et al., 2017).

The first identification of IRPL and the subsequent basic investigations into its origin were made on the Risø station for CryOgenic LUminescence Research (COLUR); this system is not convenient for routine dosimetric measurements because it is manually operated, does not include a beta source, and must be evacuated before cooling. Prasad et al. (2017) also explored the use of the spectrometer attachment to the Risø TL/OSL reader to measure IRPL for dosimetric investigations; this system is based on a spectrograph and an EMCCD camera but is relatively insensitive due to the fibre-optic coupling. Initial measurements suggested that IRPL spectra are similar across samples; hence it may be possible to modify the system to use a broad bandpass detection. This would both increases the sensitivity and cut costs.

In this article we describe new measurement systems based on IRPL detection through a wavelength bandpass, both using photomultiplier tubes (PMTs) and imaging cameras on the new automated detection and stimulation head (DASH) for the Risø TL/OSL reader (Lapp et al., 2015). DASH provides a port for an external light source and an automated filter and detector changer; this configuration gives the flexibility to allow the measurement of both IRPL and infra-red stimulated luminescence (IRSL) from the same sample. For multiple-grain IRPL measurements we use

integrated measurement using PMTs. For IRPL measurements from individual grains we either use spatially resolved measurements using an EM-CCD (Kook et al., 2015), or the single grain X-Y laser scanning system (Duller et al. 1999 and 2003), modified to reduce the IR laser power. Because the detection bandpass is close in wavelength to the light source, we must specifically address the challenge of avoiding excitation-light breakthrough into the detector. Finally we demonstrate the potential of these new measurement systems using results from a typical natural feldspar (multiple grains and single grains) samples and rock slices.

2. Instrumentation

For the development of the IRPL measurement system, we use an existing platform consisting of a standard Risø TL-DA-20 reader and DASH (Lapp et al., 2015). The DASH includes 3 software-selectable detector positions in a detector changer module and two layers of selectable filters (up to 4 in each layer). We used two PMTs and one EM-CCD camera as detectors, together with appropriate filters to allow measurement of both IRSL and IRPL in integrated or spatially-resolved mode. The different configurations are discussed below.

2.1 Detection configurations for IRPL at 880 or 955 nm

Kumar et al (these proceedings; their Figure 1) show that laser excitation at 1.49 eV (830 nm) gives rise to two IRPL emission peaks at ~1.3 eV (955 nm) and ~1.41 eV (880nm); the first emission is the same as that reported by Prasad et al. (2017) using the 1.40 (885nm) laser excitation. These authors further demonstrate that IR radioluminescence (IR-RL; Trautmann et al., 1999) and IRPL have the same emissions. The two IRPL emission peaks are resolved at low temperature (7 K), but at room temperature they merged together as a single peak. The standard PMTs (ET9245QB or PDM9107-CP-TTL) used for OSL or IRSL measurement (Bøtter-Jensen et al., 2010; Lapp et al., 2015) are not sufficiently sensitive to measure these Near-infrared (NIR)emissions. Charged couple devices (CCD) are sensitive in this wavelength range but it is usually difficult to operate a CCD or an EM-CCD in pulsed mode; this is more likely to be needed when, as here, the excitation and emission wavelengths are close to each other. A PMT detector is preferred for spatially integrated luminescence measurements as it offers the possibility of reducing background by fast gating in the presence of pulsed stimulation.

Since the IR-RL and IRPL emissions are similar, we use the PMT (Hamamatsu H7421-50) used in the IR-RL system (Buylaert et al., 2012; Lapp et al.. 2012) for detecting the 1.41 eV (880nm) IRPL

emission. This PMT has a GaAs photocathode with maximum quantum efficiency (QE) at ~830 nm gradually dropping to almost zero by ~890 nm (**Fig. 1a**). The head is thermoelectrically cooled to 0 °C for to reduce the dark counts. When the PMT is combined with two 875 nm long pass (LP) filter (Edmund optics, high performance interference filter, optical density 4) the peak of the IRPL detection window lies at 873 nm (FWHM 15 nm; **Fig. 1a**). Furthermore, the QE of the PMT extends down to 380 nm (~1.2 % at 400 nm); it is thus possible to measure IRSL using the same detector by using the automated filter changer in DASH to provide a blue band-pass filter combination (BG3 and BG39)

The ~1.3 eV (955 nm) emission from feldspar has to our knowledge never been measured using a PMT detector before. Here we use a Hamamatsu H10330C-25 with a spectral response from 950 nm to 1200 nm with a QE of ~5% (**Fig. 1b**). This PMT is contained in a thermally-insulated high vacuum housing and the internal thermoelectric cooler can reduce the temperature to -60 °C. Because of this cooling, it is possible to detect in the NIR region with <100 counts/s background count rate (for an applied voltage of 800 V). A combination of two 925 nm long pass (LP) filters (Edmund optics, high performance interference filter, optical density 4) and one 950 band pass (BP) filter (Edmund optics, high performance interference filter, optical density 4) are used in combination with this PMT to reject the excitation light and define a IRPL detection window at 950 nm (FWHM 50 nm) (Fig. 1b).

For IRPL imaging one may use a CCD detector because of their high QE to >1000 nm. Kook et al. (2015) developed a TL/OSL imaging system using a UV-enhanced EMCCD; the QE of their detector is ~40% at 880 nm and 20% at 950 nm (**Fig. 1c**). However, a broad spectral response with a high QE extending to UV poses disadvantage when measuring IRPL; unlike the PMT detector, the EMCCD is very sensitive to the excitation wavelength at 850 nm. Also, unlike the PMT, it is not possible to use pulsed laser excitation and detection only during the off-time because of the slow read-out speed of EMCCD. Thus, efficient blocking of the excitation laser becomes critical for an EMCCD-based imaging system. (It may be possible, however, to use an intensified CCD or sCMOS camera; although less sensitive overall, these do allow fast gating of the high voltage of the intensifier). Here we use the EMCCD system of Kook et al. (2015) in combination with two 925 nm long pass (LP) filters and one 950 band pass (BP) filter; this configuration gives IRPL detection from 925 to 975 nm (1.3 eV band). It was not possible to measure the 1.41 IRPL band with the EMCCD because of high breakthrough from the laser.

2.2 The IRPL attachment

A diagram of the integration of the units described into the reader head is shown in Fig. 2. The automated DASH has a port for an external light source (in addition to the built-in LEDs), and provides a control signal for external continuous or pulsed excitation (minimum 5 μs with 0.1 μs resolution). In this study we attached an IR diode laser (Power Technology incorporated, 150 mW, 830 nm) to the external port. The laser beam passes through a ground- glass diffuser to provide uniform illumination at the sample position; this reduces the power density to ~3 $mW \cdot cm^{-2}$. However, IRPL is a non-destructive measurement and so measurement at even low excitation powers can give robust counting statistics; thus, even the low optical power after diffusing the laser is sufficient for high sensitivity IRPL measurements. The objective lens (biconvex fused silica lens with anti-reflection coating) collimates the IRPL light to detectors through the detection filters (LP 875, LP 925 and BP 950/50).

The Hamamatsu H7421-50 PMT module is mounted directly on top of the DASH; a lens focuses the collimated IRPL beam from the sample to an effective measurement area of 5 mm diameter in the PMT module. In contrast, the module of Hamamatsu H10330C-25 (NIR-PMT) is bulky as it consists of a NIR-PMT main unit and a NIR-PMT unit controller; it cannot be directly placed on the DASH because of space restrictions. Thus, this module is placed beside the Risø reader and a 3 mm diameter liquid light guide (Lumatec Liquid Light Guide series 2000; transmission range of 350-2000 nm) is used to couple the third DASH detector position with the NIR-PMT. The IRPL at the end of the liquid light guide is divergent (uncollimated) and a lens is placed between the light guide and the detector to collect the IRPL photons on the photocathode (18 mm effective diameter) of the PMT.

Using the Sequence Editor control software, the detector changer locates either the PMT (H7421-50), or the liquid light guide (for H10330C-25), or the EMCCD at the measurement position. The automated filter changer then moves the appropriate filters under the chosen detector.

2.3 Rejecting the excitation light in IRPL detection

Despite using the detection filters, there is a large breakthrough from the excitation light into the PMT detectors. In order to avoid this problem we used pulsed OSL (POSL), where the excitation light is turned on and off at a fixed time interval, and the luminescence is only measured when the excitation light is off (e.g. McKeever et al., 1996; Sanderson and Clark, 1994). This technique has earlier been used to measure a quartz signal in the presence of feldspar contamination, by exploiting the different lifetimes of quartz and feldspar OSL (Thomsen et al., 2007; Ankjærgaard et al., 2010). POSL can be used to reject the breakthrough in IRPL measurement, because the switch-off time of the laser excitation pulse (< 0.1 μs) is much shorter than the IRPL lifetime of 28 μs (Prasad et al., 2017).

To optimize the PMT counting window within the off period, a time-resolved IRPL measurement was carried out using the Risø Time-Correlated Single Photon Counting (TCSPC) attachment (Lapp et al., 2009). The laser was operated using 50 μs on (pulse width) and 50 μs off time, for total of 4 seconds. **Figure 3a** shows the measurement using a blank disc and a K-feldspar (R47) disc with the H7421-50 detector (for 880 nm peak detection). A large breakthrough was observed during the on time (~1.1×10^4 s^{-1}) using a 3 mW/cm^2 optical power density on the sample position (contrast this with 140 mW/cm^2 for a classic DASH and 300 mW/cm^2 for an automated DASH for standard IRSL measurements). At least an order of magnitude higher excitation power may be used, if necessary, without risking the saturation of the PMT. The switch off time of the laser measured to be <0.1 μs (Fig. 3a inset), but there appears to be an afterglow lasting ~2 μs. Based on these data, we set the PMT counting period to begin 3 μs after the laser switch off.

Figure 3b shows TCSPC data with a NIR PMT used for measuring the 955 nm IRPL peak. In contrast to the result for the H7421-50 PMT, here the measurement of the empty disc shows that the NIR PMT is almost insensitive to the excitation laser; this is because of the very low QE at 850 nm and the sufficiently large wavelength difference between detection and excitation wavelength. The measurement of the disk containing feldspar grains shows a clear build up and decay of the 1.3 eV IRPL emission, giving a single exponential lifetime of ~ 40 μs. Thus, the 1.3 eV IRPL may be measured either using continuous wave- or pulsed-stimulation, whereas the 1.41 eV IRPL requires pulsed stimulation.

.3. IRPL measurements on feldspar extracts and rock slices

3.1 Multiple grain IRPL measurement

To illustrate the application of the IRPL measurement system, we used a SAR protocol (Murray and Wintle, 2000) on a feldspar sample (R47; detailed investigations on the sample are presented in Prasad et al., 2017). A disc of R47 initially bleached for 48 hours under Hönle solar simulator (SOL2) before measurements began. A preheat of 250 °C for 60 s was used after both the regeneration and test doses, followed by an pulsed IRPL measurement at room temperature for 5 s (on-time 50 μs; off time: 50 μs; detection in the off-time after 3 μs delay). A 395 nm UV LED (1W optical power) mounted on the reader was used for bleaching the IRPL signal before giving a test dose or a regeneration dose. A dose response curve was measured using 6 regeneration doses including a recuperation point (0 Gy) and a repeat dose (recycling point). Fig. 4a and 4b show the IRPL signals after different regenerations doses (Lx) for the 880 and 955 nm emissions, respectively. The respective dose response curves are shown inset. The L_x signals increases systematically with beta dose and the sensitivity-corrected dose response curve can be satisfactorily fitted using a single exponential function, with D_0 = 346 ±24 Gy (880 nm) and 436 ±30 Gy (955 nm).

3.2 Single grain IRPL measurement

For the single grain IRPL measurements the existing single grain system in the Risø reader (Duller et al., 2003) was adapted to use with the new detectors (H7421-50 or H10330C-25). This system already contains an IR laser (830 nm, 150 mW) for excitation, but this laser is normally operated at power density of ~500 W/cm^2 at the grain to maximise the signal to noise ratio. The same power density is not necessary for IRPL; this nearly time invariant signal is orders of magnitude more intense that IRSL and can also be measured over a prolonged period to increase the signal-to-noise ratio. In addition, a very intense IR laser stimulation power may also heat the grain during measurement. To minimise these effects, we reduced the laser power by a factor of ~ 100 using a neutral density filter (OD2). To reduce the breakthrough of excitation light, we also modified the existing stimulation control in the single grain system to allow pulsed IR stimulation. For single grain measurement, the laser was pulsed with a 5 μs on-time and 95 μs off-time, and signal was accumulated by the PMT for 92 μs during the off time, after a delay of 3μs.

Figure 5 shows the results of the IRPL-SAR dose recovery measurements using two single grain discs of a calibration feldspar sample (Hansen et al., these proceedings) given an *in-situ* beta dose of

90 Gy in the Risø reader. A preheat 280 °C for 60 s was used prior to the measurement of the IRPL signals (for both regeneration and test dose). Optical bleaching at 260 °C using the blue LEDs was used to reset the IRPL before the next measurement both within and at the end of a SAR cycle. Figure 5a shows the IRPL signals from a typical grain (with above average brightness) after a given dose of 90 Gy, a regeneration dose of 45, 90, 180, 0 and 90 Gy, and the background IRPL (after bleaching) at the end of the first SAR cycle. The IRPL curves were flat (non decaying) for most grains; a few grains showed up to 10% decay in the 5 s stimulation period. Figure 5b, shows the SAR dose response curve from the same grain, and Figure 5c the normalised test-dose as a function of SAR cycle. This particular grain shows negligible sensitivity change (a common but not universal observation). Figure 5d shows a histogram of the recovered doses; the measured to given dose recovery ratio based on 132 accepted grains was 1.004±0.014.

3.3 IRPL imaging system.

Figure 6 shows the results obtained using the IRPL imaging system. Figure 6a and 6b show the optical and IRPL image, respectively, following 105 Gy dose to a feldspar single grain disc (sample R47). The IRPL signal was integrated for 5 s; the IRPL signal was constant with time, whereas the IRSL decayed during the 5 s stimulation. Because of this, the IRPL sensitivity can be increased arbitrarily by increasing the integration time. In this particular data set (Figure 6a), grain 43 gave an IRPL count rate of 1.3×10^5 s^{-1} and grain 45 gave 5.4×10^5 s^{-1}. These high count rates also allow the use of a smaller optical aperture to improve image resolution and so reduce cross talk.

Figure 6c shows the optical image of a granite rock slice (from an archaeological stone pier near Fyn, Denmark). A corresponding data set for the mineralogical composition (K-F, Ca-F and NA-F) was obtained using X-ray fluorescence (μXRF; Bruker, Tornado M4) (Figure 6b); the red areas in this figure are rich in potassium, presumably in potassium feldspar. Figure 6e shows the IRPL image of the same slice; it appears that the IRPL is strongly correlated with the potassium-rich areas.

3. Conclusion

We have demonstrated a new measurement system for detecting infrared photoluminescence (IRPL) emissions at ~1.41 eV (880 nm) and ~1.3 eV (955 nm). The system uses an external light source at 1.49 eV (830 nm) and three detectors based on PMTs or and EMCCD (coupled to appropriate filters), all mounted on the automated DASH unit in the Risø TL/OSL reader. Pulsed stimulation

using the PMT detectors proves to be useful to reject excitation light breakthrough, especially in case of the 1.49 eV emission. We demonstrate the potential of the PMT based system for dosimetric investigations using pulsed IRPL on both multiple-grain and single-grain measurement systems. Using the latter, we gave a calibration feldspar a known dose of 90 Gy, and measured 90.4 ±1.3 Gy.

We also demonstrate the potential of IRPL (1.3 eV) for imaging using a single grain disc and a rock slice; these measurements used CW-IR stimulation and EMCCD detector. A strong correlation between the IRPL and K-feldspar concentration is inferred based on the μXRF measurements on the same granite slice.

In order to further develop IRPL imaging future effort will concentrate on either rejecting the excitation light more efficiently by the use of filters or using pulsed stimulation, or alternatively reducing the image area using, for example, microscopic techniques. Furthermore, since very low excitation light power is required, high resolution imaging of large samples is straightforward. This is particularly relevant for rock surface dating (Sohbati et al., 2015; Freiesleben et al., 2015)

References

L. Bøtter-Jensen, S.W.S. McKeever, A.G. Wintle, 2003. Optically Stimulated Luminescence Dosimetry. Elsevier, Amsterdam.

A. K. Prasad, N. R.J. Poolton, M. Kook, and M. Jain, 2017. Optical Dating in a New Light: A Direct, Non-Destructive Probe of Trapped Electrons. Scientific Reports 7 (1). Springer US:1–15. https://doi.org/10.1038/s41598-017-10174-8.

R. Kumar, A.K. Prasad, M. Kook, A.S. Murray, M. Jain, (these proceedings) Towards direct measurement of metastable (trapped) electrons in K-feldspar: Do infrared- photoluminescence (IRPL) and radioluminescence (IR-RL) probe the same trap(s) ?

T. Lapp, M. Kook, A.S. Murray, K.J. Thomsen, J.-P. Buylaert, M. Jain, 2015. A new luminescence detection and stimulation head for the Risø TL/OSL reader. Radiat. Meas. 81, 178-184

T. Trautmann, M.R. Krbetschek, A. Dietrich, and W. Stolz, 1999. Feldspar Radioluminescence: A New Dating Method and Its Physical Background. Journal of Luminescence 85 (1–3):45–58. https://doi.org/10.1016/S0022-2313(99)00152-0.

L. Bøtter-Jensen, K.J. Thomsen, M. Jain, 2010. Review of optically stimulated luminescence (OSL) instrumental developments for retrospective dosimetry. Radiat. Meas. 45, 253-257.

M. Kook, T. Lapp, A.S. Murray, K.J. Thomsen, M. Jain, 2015. A luminescence imaging system for the routine measurement of single-grain OSL dose distributions, Radiat. Meas. 81, 171-177

G.A.T. Duller, L. Bøtter-Jensen, A.S. Murray, A.J. Truscott, 1999. Single grain laser luminescence (SGLL) measurements using a novel automated reader. Nucl. Instrum. Methods Phys. Res. Sect. B. 155 (4), 506-514

G.A.T. Dullera, L. Bøtter-Jensen, A.S. Murray, 2003. Combining infrared- and green-laser stimulation sources in single-grain luminescence measurements off feldspar and quartz, Radiat. Meas. 37, 543 – 550

J.-P. Buylaert, M. Jain, A.S. Murray, K.J. Thomsen, T. Lapp, 2012. IR-RF dating of sand-sized K-feldspar extracts: A test of accuracy, Radiat. Meas. 47, 759-765

Torben Lapp, Mayank Jain, Kristina J. Thomsen, Andrew S. Murray, Jan-Pieter Buylaert, 2012. New luminescence measurement facilities in retrospective dosimetry, Radiat. Meas. 47, 803-808

S.W.S. McKeever, B.G. Markey, M.S. Akselrod, 1996. Pulsed optically stimulated luminescence dosimetry using a-Al2O3:C. Radiat. Protect. Dosimetry 65, 267–272.

D.C.W. Sanderson, R.J. Clark, 1994. Pulsed photostimulated luminescence of alkali feldspars. Radiation Measurement 23, 633–639.

K.J. Thomsen, M. Jain, A.S. Murray, P.M. Denby, N. Roy, L. Bøtter-Jensen, 2008. Minimizing feldspar OSL contamination in quartz UV-OSL using pulsed blue stimulation, Radiat. Meas. 43, 752 – 757

C. Ankjærgaard, M. Jain, K.J. Thomsen, A.S. Murray, 2010. Optimising the separation of quartz and feldspar optically stimulated luminescence using pulsed excitation. Radiat. Meas. 45, 778-785.

T. Lapp, M. Jain, C. Ankjærgaard, L. Pirtzel, 2009. Development of pulsed stimulation and Photon Timer attachments to the Risø TL/OSL reader, Radiat. Meas. 44 571–575

A.S. Murray, A.G. Wintle, 2000. Luminescence dating of quartz using an improved single-aliquot regenerative-dose protocol. Radiat. Meas. 32, 57–73.

R. Sohbati, , A.S. Murray, N. Porat, M. Jain, U. Avner, 2015. Age of a prehistoric “Rodedian” cult site constrained by sediment and rock surface luminescence dating techniques. Quat. Geochronol. 30, 90–99

T. Freiesleben, , R. Sohbati, A.S. Murray, M. Jain, S. A. Khasawneh, , S. Hvidt, B. Jakobsen, 2015. Mathematical model quantifies multiple daylight exposure and burial events for rock surfaces using luminescence dating. Radiat. Meas. 81, 1–7

Figure Captions

Fig. 1 (a) Quantum efficiency of H7421-50 PMT (black dot), 830 nm excitation laser (red line (b) Quantum efficiency of H10330C-25 PMT (black dot). (c) Quantum efficiency of EMCCD (black dot). All three figures also present transmission characteristics of the relevant long pass interference filters (magenta dash dot; see legend) and the IRPL emission spectrum (blue) at room temperature; these data refer to the left hand axis. Filter transmittance was recorded with Shimadzu spectrophotometer (UV-2600/2700).

Fig. 2. Schematic diagram showing the components of the IRPL measurement system mounted on the Risø TL/OSL reader.

Fig. 3 (a) Time-resolved IRPL signals using the H7421-50 PMT from feldspar (black cure) and a blank disc (red dash). These curves were produced by summing signals from all the pulses produced in 4 s, using an On time of 50 μs and an Off-time 50 μs at room temperature. Note that the y axis is on log scale. (b) Time-resolved IRPL signal with the H10330C-25 PMT from feldspar (black line) and blank disc (red dash) using the same configuration as in (a).

Fig. 4 (a) IRPL (1.41 eV; 880 nm emission) signals in response to increasing regeneration dose. The inset shows the corresponding SAR dose response curve. (b) IRPL (1.3 eV; 955 nm emission) signals in response to increasing regeneration dose. The inset shows the corresponding dose SAR response curve.

Fig. 5. Dose recovery for IRPL (1.3 eV; 955 nm emission) using the single grain attachment. A) IRPL curves from the given 90 Gy dose, a 45, 90, 180, 0 and 90 Gy regeneration dose, and the background IRPL at the end of the first SAR cycle, b) the dose response curve for the same grain as shown in (a). (c) the normalised sensitivity of the test dose signal during the different SAR cycles from the same grain as in (a). (d) A histogram of the recovered doses based on 132 accepted grains.

Fig. 6. (a) The optical image of a feldspar (R47) single-grain disc under low power IR illumination (b) IRPL image of the same disc following a beta dose of 105 Gy; the integration time for IRPL was 5 s. (c) optical image of a granite rock slice. (d) Compositional image of the same rock slice showing K-F, Na-F and Ca-F rich areas; the image was measured using μXRF. (e) IRPL image of the same rock slice following a beta dose of 100 Gy. The integration time for IRPL was 10 s.

Fig. 1

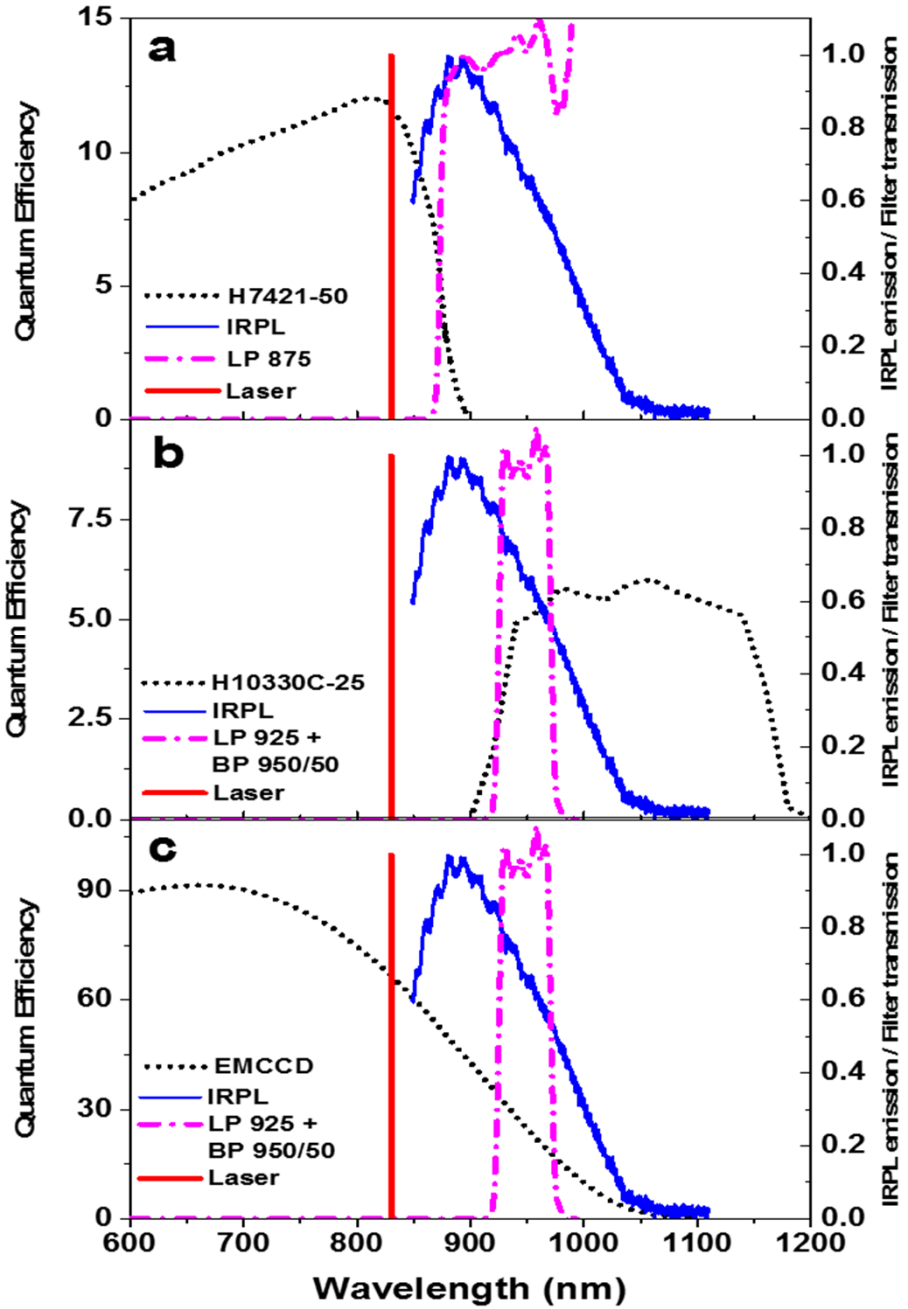
a
Quantum Efficiency
IRPL emission / Filter transmission
H7421-50
IRPL
LP 875
Laser
b
H10330C-25
IRPL
LP 925 +
BP 950/50
Laser
c
EMCCD
IRPL
LP 925 +
BP 950/50
Laser
Wavelength (nm)

Fig. 2

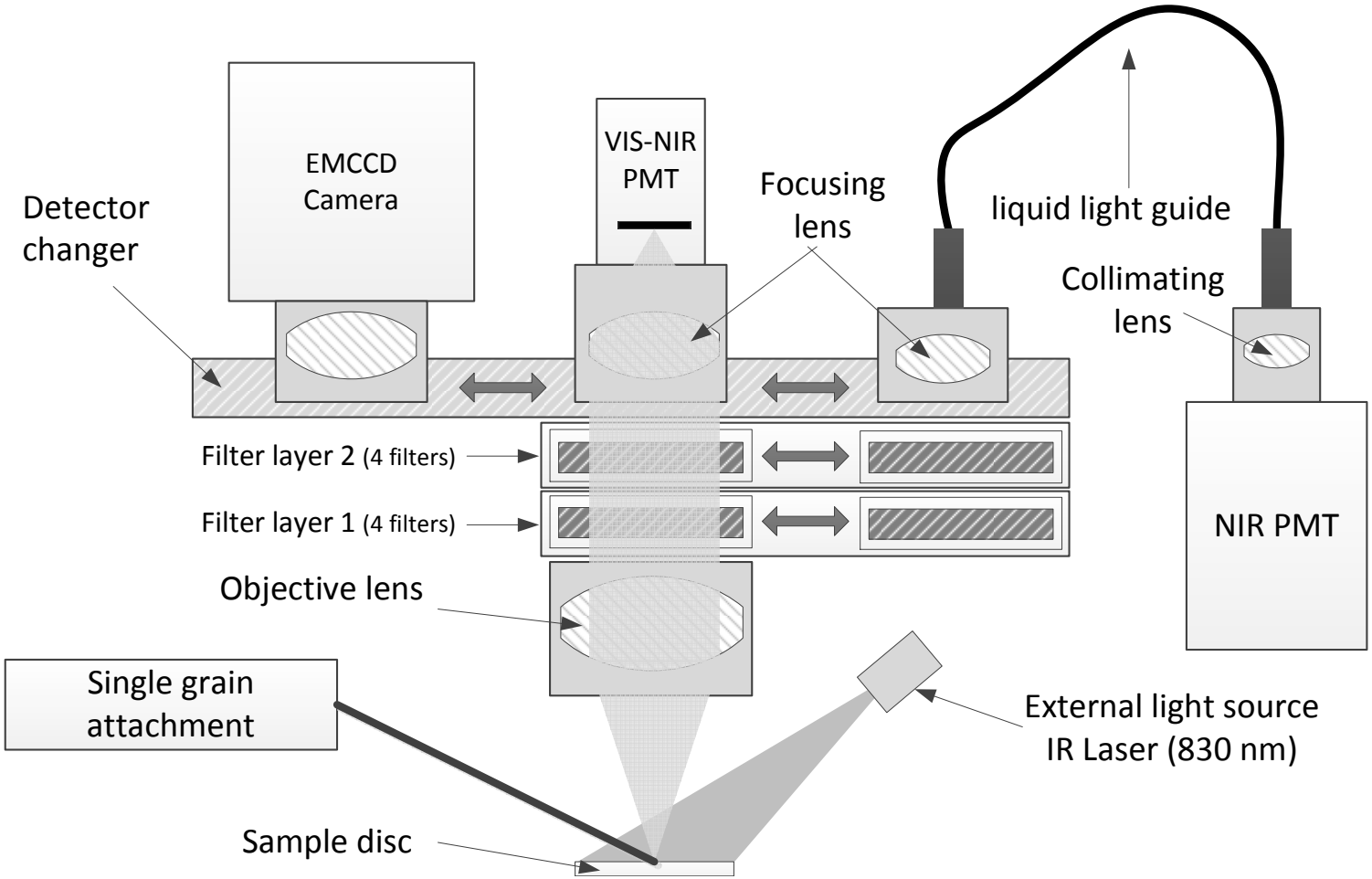
EMCCD
Camera
VIS-NIR
PMT
Detector
changer
Focusing
lens
liquid light guide
Collimating
lens
Filter layer 2 (4 filters)
Filter layer 1 (4 filters)
NIR PMT
Objective lens
Single grain
attachment
External light source
IR Laser (830 nm)
Sample disc

Fig. 3

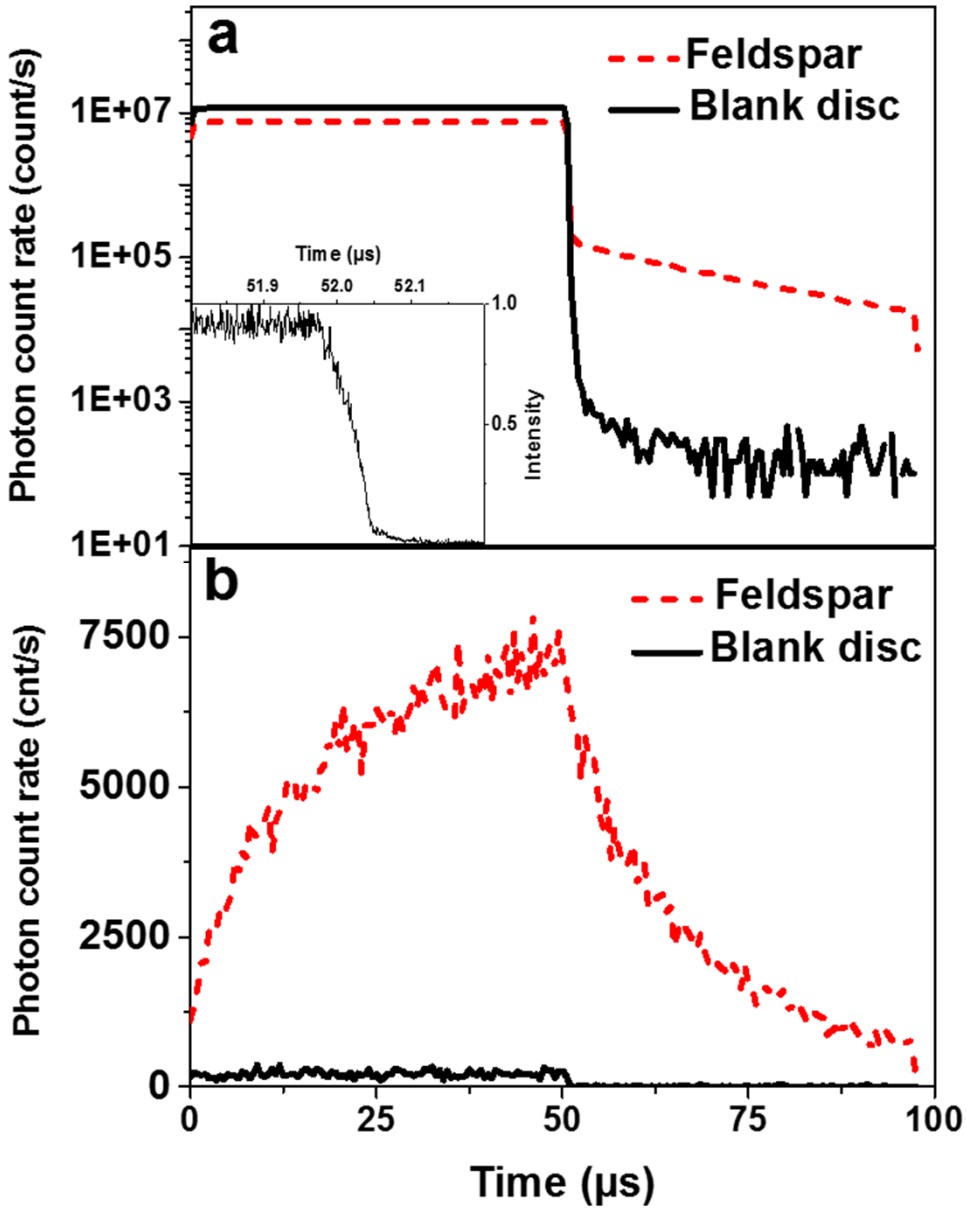

Fig. 4

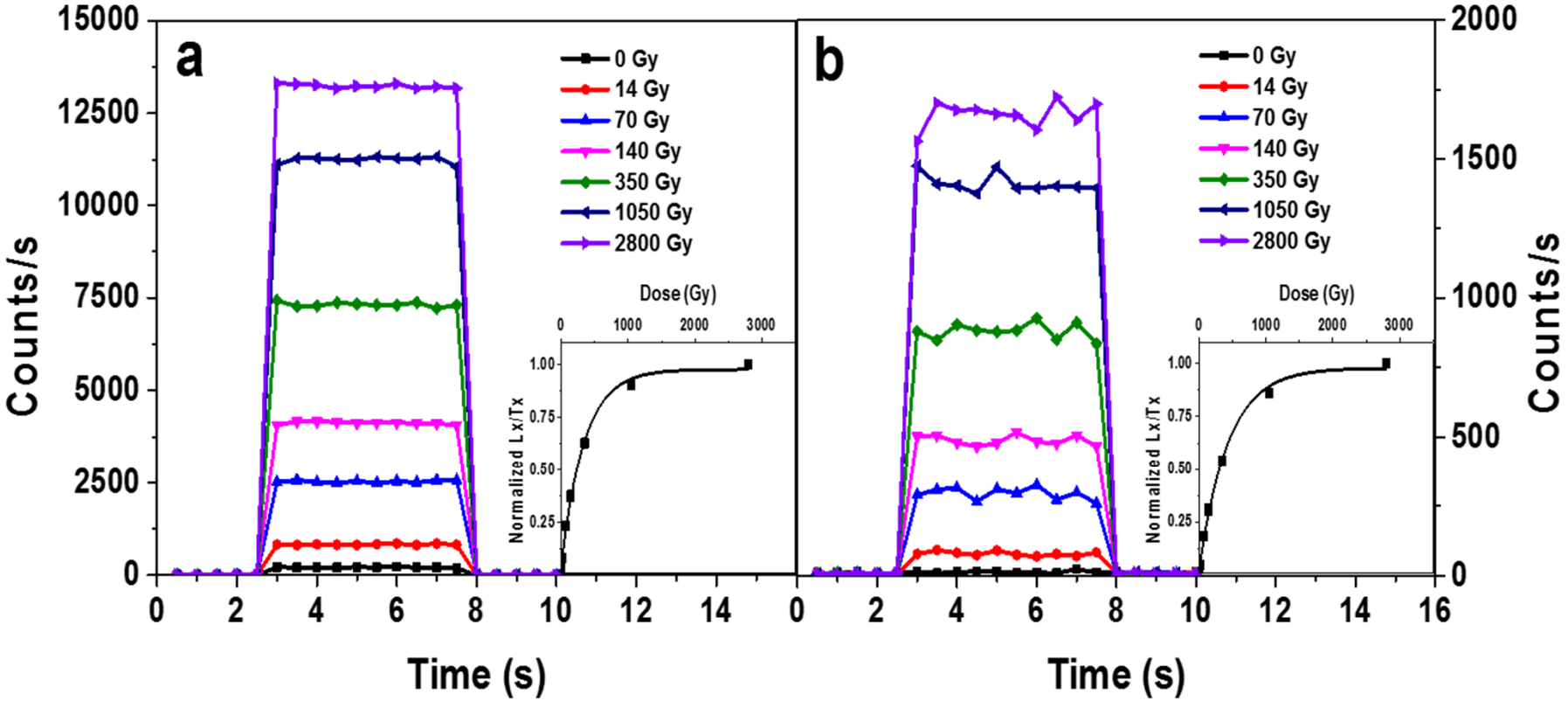
a
b
0 Gy
14 Gy
70 Gy
140 Gy
350 Gy
1050 Gy
2800 Gy
Counts/s
Time (s)
Dose (Gy)
Normalized Lx/Tx

Fig. 5

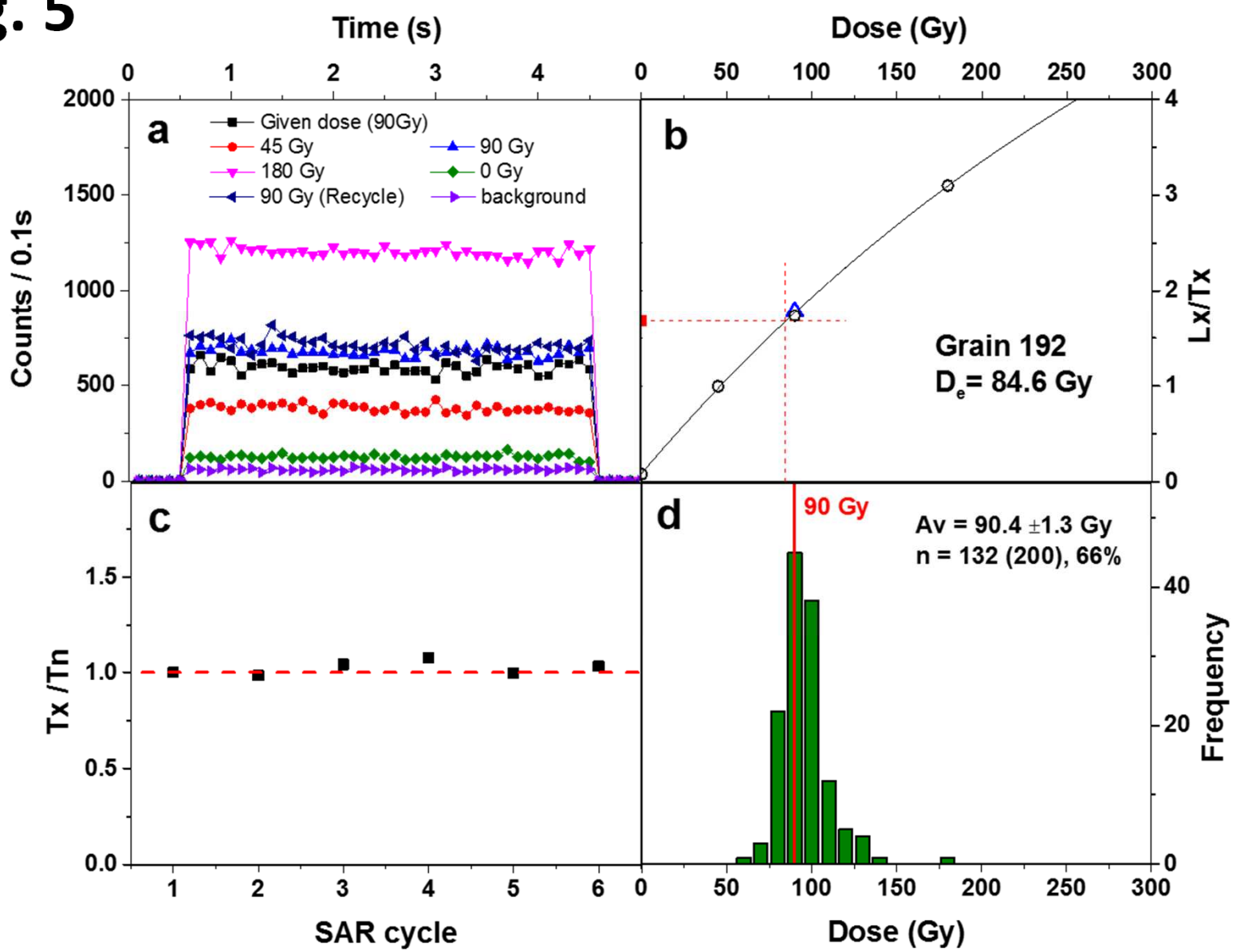
Time (s)
Dose (Gy)
a
b
c
d
Given dose (90Gy)
45 Gy
90 Gy
180 Gy
0 Gy
90 Gy (Recycle)
background
Counts / 0.1s
Lx/Tx
Grain 192
De= 84.6 Gy
90 Gy
Av = 90.4 ±1.3 Gy
n = 132 (200), 66%
Tx /Tn
Frequency
SAR cycle
Dose (Gy)

Fig. 6

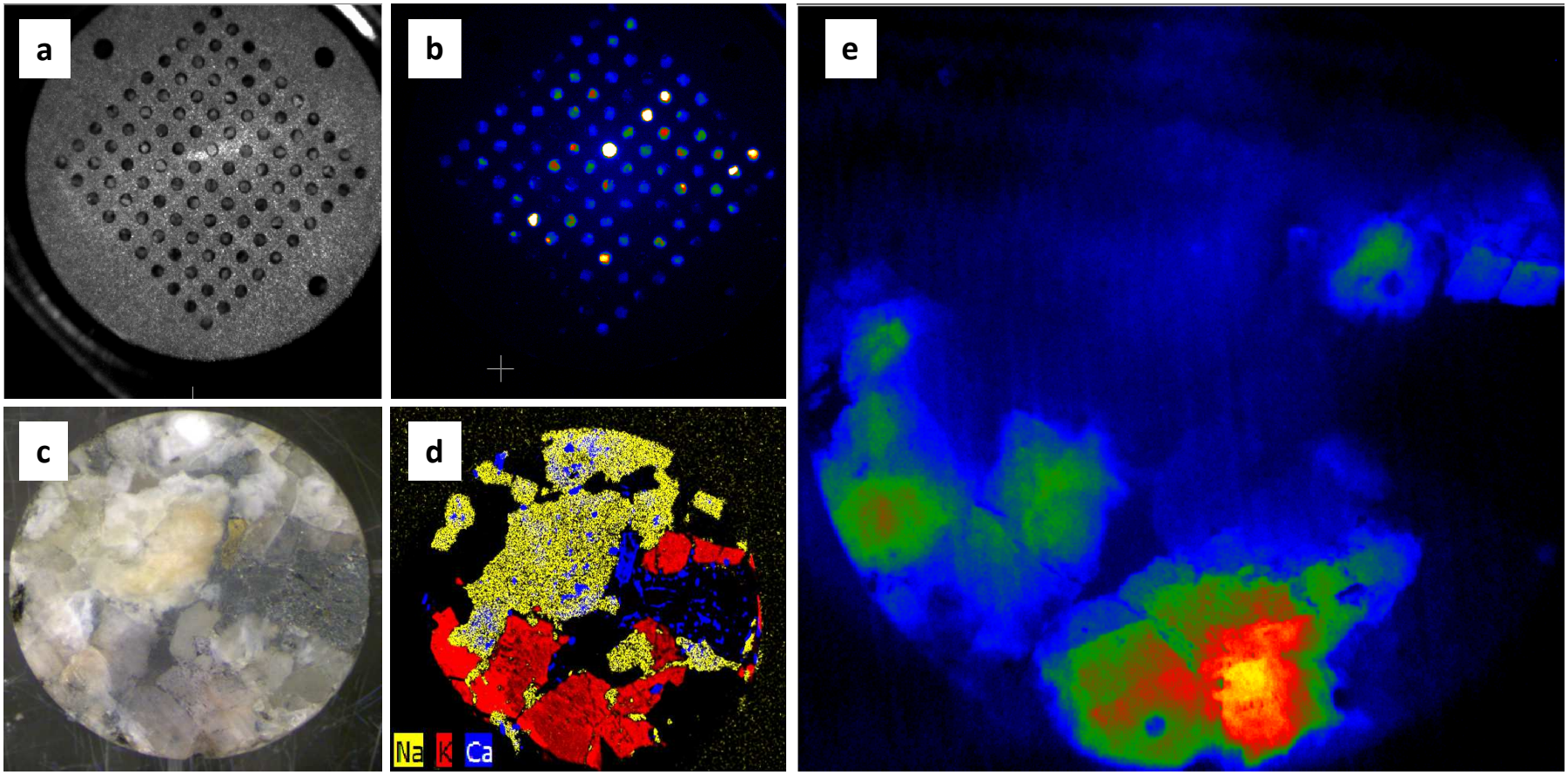

Highlights

1. Describing a measurement system for infrared photoluminescence (IRPL)

2. Characterizing the performance of the IRPL measurement system

3. Spatially resolved IRPL measurements